

# Conduction Deficits and Membrane Disruption of Spinal Cord Axons as a Function of Magnitude and Rate of Strain

Riyi Shi and Jim Whitebone

*Department of Basic Medical Sciences, The Institute for Applied Neurology, School of Veterinary Medicine, and Weldon School of Biomedical Engineering, Purdue University, West Lafayette, Indiana*

Submitted 4 April 2005; accepted in final form 21 February 2006

**Shi, Riyi and Jim Whitebone.** Conduction deficits and membrane disruption of spinal cord axons as a function of magnitude and rate of strain. *J Neurophysiol* 95: 3384–3390, 2006. First published March 1, 2006; doi:10.1152/jn.00350.2005. White matter strips extracted from adult guinea pig spinal cords were subjected to tensile strain (stretch) injury *ex vivo*. Strain was carried out at three magnitudes (25, 50, and 100%) and two strain rate regimens: slow (0.006–0.008 s<sup>-1</sup>) and fast (355–519 s<sup>-1</sup>). The cord samples were monitored physiologically using a double sucrose-gap technique and anatomically using a horseradish peroxidase assay. It seems that a higher magnitude of strain inflicted significantly more functional and structural damage within each strain rate group. Likewise, a higher strain rate inflicted more damage when the strain magnitude was maintained. It is evident that axons have remarkable tolerance to strain injury at a slow strain rate. Even a 100% strain at the slow rate only eliminated two-thirds of the compound action potential amplitude and resulted in almost no membrane damage when examined 30 min after strain. It is also clear that the spontaneous recovery is evident yet not complete compared with preinjury levels at the fast strain rate. To examine the factors that might influence the vulnerability of axons to strain, we have shown that the axonal diameters did not play a significant role in dictating the susceptibility of axons to strain. Rather, it is speculated that the location of axons might be a more important factor in this regard. The knowledge gained from this study is likely to be informative in elucidating the spinal cord biomechanical response to strain and strain rate.

## INTRODUCTION

There is little doubt that most devastating functional deficits in traumatic spinal cord injury stem from damage to axons of the white matter. Injury of these axons could result in partial or complete loss of sensory and motor function below the injury level (Anderson and Hall 1993; Honmou and Young 1995). A better understanding of axonal pathology as a result of mechanical insults should help in comprehending the underlying mechanisms of functional damage and recovery and perhaps the development of therapeutic interventions.

Longitudinal strain of spinal cord axons is a significant component of compression injury when force is exerted laterally, a common form of mechanical insult in spinal cord injury (Blight 1988; Blight and DeCrescito 1986). Furthermore, evidence suggests that axons are sensitive to strain and localized regions of high strain may be detrimental (Blight and DeCrescito 1986; Shi and Pryor 2002). For example, during a moderate lateral compression, the onset of injury occurs in axons located in the middle of the spinal cord where significant

longitudinal strain is expected (Shi and Pryor 2002). On the other hand, when a cord segment is stretched, most axonal damage occurs in the outer realm of the cord where the elongation of axons is expected to be the most severe (Shi and Pryor 2002). Moreover, in a rat vertebral dislocation model of spinal cord injury, it was shown that the most severe axonal injury coincided with the area of greatest regional strain (Fiford et al. 2004). In summary, it is likely that tensile strain injury is an important component of mechanical trauma of the spinal cord.

To study the functional and structural significance of tensile strain injury, we have developed an *ex vivo* model using isolated guinea pig spinal cord white matter (Shi and Pryor 2002). Using this model, we have shown that longitudinal strain can inflict significant functional and morphological deficits (Shi and Pryor 2002). However, the detailed knowledge concerning the damage to axons as a function of the magnitude and the rate of strain has not yet been obtained. In this regard, we have chosen to study strain injury at two distinct strain rates: slow (0.006–0.008 s<sup>-1</sup>) and fast (355–519 s<sup>-1</sup>).

This study was designed to investigate the impulse conduction and accompanying membrane disruption as functions of three magnitudes of strain at two strain rates in an established *ex vivo* model. Functional changes were monitored by double sucrose gap recording device, and structural damages were assessed by a horseradish peroxidase (HRP) exclusion test. We have found that, in addition to the magnitudes, the strain rate also plays a significant role in inflicting functional and anatomical deficits.

## METHODS

### *Isolation of spinal cord*

The experimental protocols have been reviewed and approved by the Purdue University Animal Care and Use Committee (PACUC). A total of 55 guinea pigs were used for this study. The technique for isolation of the spinal cord was similar to that described previously (Jensen and Shi 2003; Shi and Blight 1996; Shi and Borgens 1999). Adult female guinea pigs of 350- to 500-g body weight were used. After anesthesia, the animal was perfused transcatheterially with cold (15°C) Krebs' solution, and the vertebral column was rapidly excised. The laminae from the lumbo-sacral to cervical levels were removed in a continuous strip by cutting through the pedicles on either side with malleus nippers. The roots were cut carefully with microscissors as the cord was gently removed from the inverted vertebral column and placed in cold Krebs' solution [composed of (in mM) 124 NaCl, 5

Address for reprint requests and other correspondence: R. Shi, Center for Paralysis Research, Dept. of Medical Sciences, School of Veterinary Medicine, Purdue Univ., West Lafayette, IN 47907 (E-mail: riyi@purdue.edu).

The costs of publication of this article were defrayed in part by the payment of page charges. The article must therefore be hereby marked "advertisement" in accordance with 18 U.S.C. Section 1734 solely to indicate this fact.

KCl, 1.2 KH<sub>2</sub>PO<sub>4</sub>, 1.3 MgSO<sub>4</sub>, 2 CaCl<sub>2</sub>, 20 dextrose, 26 NaHCO<sub>3</sub>, and 10 sodium ascorbate, equilibrated with 95% O<sub>2</sub>-5%CO<sub>2</sub>). The cord was separated first into two halves by a midline sagittal division. The ventral white matter was obtained by separating it from the gray matter with a scalpel against a soft plastic block (Fig. 1A). To ensure recovery from dissection, white matter strips were maintained in continuously oxygenated Krebs' solution for at least 1 h before mounting in the recording chamber.

### Electrophysiological recording

The construction of the recording chamber and the arrangement of isolated spinal cord white matter have been described in previous publications (Jensen and Shi 2003; Shi and Blight 1996; Shi and Pryor 2002). Briefly, a strip of spinal cord white matter ~42 mm in length and ~1.5 mm in diameter was placed across the chamber with the central compartment receiving a continuous perfusion of oxygenated Krebs' solution maintained at 37°C. The free ends of the white matter strip were placed across the sucrose gap channels to side compartments filled with isotonic (120 mM) potassium chloride. The sucrose gap was perfused with isotonic sucrose (320 mM) solution at a rate of 1 ml/min. The white matter strip was sealed with a thin plastic piece and vacuum grease on either side of the sucrose gap channels to prevent the exchange of solutions. The axons were stimulated and

compound action potentials (CAPs) were recorded at opposite ends of the strip by silver-silver chloride wire electrodes positioned within the side and central compartments. Stimuli were delivered in the form of 0.1-ms constant current unipolar pulses. Recordings were made using a bridge amplifier (Neurodata Instruments), and subsequent analysis was performed using custom Labview software (National Instruments) on a Dell PC. Further details and a description of the original chamber can be found in our previous publications (Jensen and Shi 2003; Shi and Blight 1996; Shi and Borgens 1999; Shi and Pryor 2002).

For the recording of CAP amplitude, stimuli were delivered at a frequency of one stimulus every 3 s. A supramaximal stimulus (110% of the maximal stimulus) intensity was chosen for this test. The digitized profile of each responding CAP was recorded continuously and stored in the computer for later analysis. In addition, a real-time plot of CAP amplitude was also displayed during the experiment (Shi and Blight 1996; Shi and Borgens 1999; Shi and Pryor 2002).

Because axons with different diameters require different thresholds to evoke an action potential in response to stimulation (BeMent and Ranck 1969; West and Wolstencroft 1983), we analyzed axonal responses to changing stimulus. Current-voltage tests, which consist of a series of stimuli with increasing intensity, can gradually stimulate axons of different thresholds to fire action potentials. The larger diameter axons will theoretically tend to be activated first, at a given stimulus intensity (Kandel et al. 2000). This test was used to detect changes in activation threshold (probability) before and after 4-AP application (Jensen and Shi 2003). The stimulus intensities ranged from 1.85 to 6.5 V. At each stimulus intensity level, five stimuli were repeated, and an average value was used.

### Strain injury

The device used to induce strain injury and the estimation of the magnitude of strain (the degree of elongation from the initial length) are described in our previous publications (Jensen and Shi 2003; Shi and Pryor 2002). As shown in Fig. 1B, a flat raised surface with a small hole was placed in the center compartment of the double sucrose gap recording chamber. The ventral white matter strip to be strained was immobilized across the surface with a nylon mesh stabilizer on either side of the elongation site. The magnitudes of strain was determined using the following equation

$$\epsilon = \frac{c - a}{a} = \frac{\sqrt{a^2 + b^2} - a}{a}$$

where  $\epsilon$  is strain value,  $a$  is the distance between the edge of the nylon mesh stabilizer and the center of the strain rod (prestrain length),  $b$  is the vertical distance between the tip of the strain rod and the level of nylon mesh stabilizer,  $c$  is the distance between the edge of the nylon stabilizer and the tip of the strain rod (strained length) (Fig. 1, B and C). The severity of the strain injury described here (mild, moderate, and severe) is obviously model-specific and was not attempted to correlate with any clinical classifications of spinal cord trauma.

The strain rod traveled at a rate of either 25  $\mu$ m/s (slow) or 1.5 m/s (fast), producing either slow or fast strain. In the slow strain rate, the movement of the strain rod was produced using a slow moving motorized micromanipulator. In the fast strain rate, the rod motion was created by its free fall in addition to being spring loaded. Thus the velocity ( $v$ ) of the rod was determined by the vertical distance ( $h$ ) it traveled, the mass of the strain rod ( $m$ ), acceleration of gravity ( $g$ ), and the work ( $W$ ) required to move the strain rod to desired height. The mass  $m$  was measured to be 0.3172 kg, and  $W$  was calculated from the spring constant (92 N/m) and the amount of spring prestretch from its natural undeformed position.

Velocity of strain rod before impact was computed using conservation of energy principles

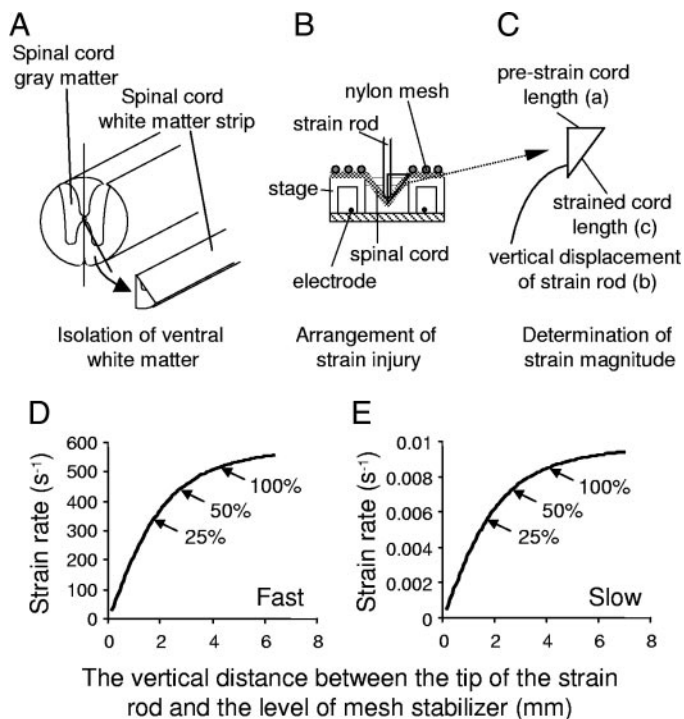


FIG. 1. Diagram showing isolation of spinal cord white matter strips, strain injury device, and determination of strain rate. *A*: steps to isolate white matter strips from adult guinea pig spinal cord. *B*: isolated white matter strip is mounted in the double sucrose gap recording apparatus. Shown here is the lateral view of central well outlining the apparatus used to inflict strain injury on isolated spinal cord ventral white matter. A strain injury is produced with a premeasured drop (slow or fast) of a Plexiglas rod onto the center of the cord strip. The strip was immobilized on either side before strain by nylon mesh, placed on the cord surface. Tissue was maintained at 37°C in the central well. *C*: higher magnification of the cord segment that is strained (as schematic of right triangle) in *B* is shown. This right triangle is used to calculate length of the injury segment after strain (*c*). Prestrained cord length is represented by *a* and vertical displacement of strain rod by *b*. *D* and *E*: graphics display changes of strain rate as a function of distance traveled by strain rod. Note that asymptotic shape of curve indicating strain rate tends to reach a constant level as the distance between the tip of the strain rod and the level of mesh stabilizer grows.

$$mgh + W = \frac{1}{2}mv^2$$

Then

$$v = \sqrt{\frac{2(mgh + W)}{m}}$$

it can be shown that when the rod is allowed to travel vertically for 40 mm, the speed of the rod at the time of contacting cord will be around 1.5 m/s. With a fixed traveling distance for the rod, we can further adjust the starting (or ending) position of strain rod so the tip of the rod (at its lowest level) can produce strain at magnitudes of 25, 50, and 100% (Shi and Pryor 2002).

#### Determination of strain rate

The strain rate is a parameter describing how fast a sample is strained (or stretched) in reference to its original length. Therefore strain rate is defined as the percent of change in length per second ( $s^{-1}$ ). For example,  $1 s^{-1}$  means that an object is elongated at a speed of 100% of its original length per second.

The cord strain rate is a function of strain rod position and can be estimated based on the known parameters (Fig. 1B). Using the above-mentioned method, we have calculated that in the fast strain (when the velocity of the rod was about 1.5 m/s), the strain rate at the points of mild (25%), moderate (50%), and severe (100%) strain are 355, 443, and  $519 s^{-1}$ , respectively (Fig. 1D). Likewise, in the slow strain regimen, the strain rates at the points of mild, moderate, and severe strain are 0.006, 0.007, and  $0.008 s^{-1}$ , respectively (Fig. 1E). This shows that the strain rate was not the same at the magnitudes of 25, 50, and 100%. However, when compared as two groups, fast and slow, the differences in strain rate are much greater between groups than within groups.

#### HRP exclusion test

HRP exclusion tests were performed based on methods described previously (Shi 2004; Shi and Borgens 1999; Shi and Pryor 2002). Briefly, white matter strips were transferred after strain to oxygenated Krebs' solution containing 0.015% HRP. After incubation for 1 h at room temperature, the tissue was fixed by immersion in 2.5% glutaraldehyde in a phosphate buffer. Transverse sections of the tissue within the injury site (Fig. 1B) were cut at  $30 \mu m$  on a vibratome and processed with diaminobenzidine by conventional methods to reveal the extent of HRP uptake in the damaged axons (Shi 2004; Shi and Borgens 1999; Shi and Pryor 2002). Digital images were taken using an Optronics video camera and National Institutes of Health Image software on a Macintosh computer. Histological sections from the strained cords at various injury combinations and control cords were examined (Fig. 3, A–E). These latter sections helped to establish a control group for the presence of HRP in damaged fibers that might be unrelated to those deliberately injured. In addition, histological sections obtained immediately after transection were also examined to reveal the background HRP labeling. This was accomplished by exposing the cut end of the axons to HRP immediately after transection. It has been shown that it takes 30–60 min for the damaged axons within a transected cord to completely reseal (Shi et al. 2000). Therefore immediate exposure of HRP after transection could result in HRP labeling of most, if not all, the axons. This group helped determine the sensitivity of the dye exclusion technique by providing data on the maximum number of axons that could be detected, counted, and grouped by caliber spectra.

#### Statistic methods

ANOVA and Tukey tests were used in all the data analysis, with a significance level chosen at  $P < 0.05$ . Linear correlation was ex-

pressed by Pearson correlation coefficient ( $r$ ). Averages were expressed in mean  $\pm$  SE.

## RESULTS

### Conduction deficits as a function of the magnitude and rate of strain

The CAP was monitored continuously before and after strain. The CAP amplitude at  $\sim 30$  min after strain was taken as the final recovered CAP. As indicated in Fig. 2, with both slow and fast strain rates, strain inflicted a significant decrease of CAP amplitude as a function of strain magnitude. Similar to our previous report (Jensen and Shi 2003; Shi and Pryor 2002), the CAP amplitude decreased immediately on strain and slowly recovered until the amplitude reached a plateau at  $\sim 30$  min after injury (Fig. 2). For example, slow-mild, moderate, and severe strain modes decreased CAP amplitude to  $99.1 \pm 1.9$ ,  $78.1 \pm 1.7$  and  $33.3 \pm 1\%$  of prestrain levels, respectively, when measured 30 min after injury ( $n = 8$  in each group). In a similar experimental setting, the mild, moderate, and severe strain in the fast mode decreased CAP to  $29.1 \pm 1.7$ ,  $18.5 \pm 1.7$ , and  $2.6 \pm 0.7\%$  of preinjury level, respectively, when measured 30 min after strain ( $n = 8$  in each group). At each strain magnitude (mild, moderate, and severe), the fast strain consistently inflicted significantly more conduction loss than slow strain ( $P < 0.001$ ). Likewise, at both fast and slow strain modes, an increase in strain magnitude significantly inflicted more conduction loss ( $P < 0.05$  to  $P < 0.001$ ). It is interesting to point out that the fast-mild strain produced a similar level of CAP amplitude loss as slow-severe strain ( $P > 0.05$ ), further showing that strain rate plays a significant role in decreasing CAP amplitude.

### Axon permeability changes in response to strain

In addition to CAP amplitude loss, strain also inflicted significant membrane disruption as a function of strain rate and strain magnitude, signified by the HRP exclusion test. As indicated in Fig. 3, fast-moderate and fast-mild strains resulted in a significant increase of HRP-labeled axons at both 0 ( $2,455 \pm 171$  and  $1,909 \pm 173$  axons/ $mm^2$ , respectively) and 30 min after strain ( $913 \pm 102$  and  $464 \pm 22$  axons/ $mm^2$ , respectively), even though partial membrane resealing is evident at this point. All these values are significantly higher than that of control cords ( $12 \pm 2$  axons/ $mm^2$ ,  $P < 0.05$  to  $P < 0.001$ ). Furthermore, increasing the magnitude of strain from mild to moderate resulted in a significant increase of HRP-labeling at both 0 ( $P < 0.001$ ) and 30 min after strain ( $P < 0.05$ ). On the other hand, slow strain produced less overall HRP labeling. Specifically, slow-severe and slow-moderate strains produced an HRP labeling of  $871 \pm 116$  ( $P < 0.001$  compared with control,  $n = 8$ ) and  $217 \pm 54$  axons/ $mm^2$  ( $P < 0.05$  compared with control,  $n = 8$ ) immediately after strain. Also, HRP labeling of slow-severe strain is significantly higher than that of slow-moderate when examined immediately after strain ( $P < 0.001$ ). At 30 min after strain, however, the value of HRP labeling of both slow-severe and slow-moderate strain recovered to values that are not significantly different from that of control ( $22 \pm 6$  and  $12 \pm 4$  axons/ $mm^2$ , respectively;  $P > 0.05$  compared with control; Fig. 3). Slow-mild strain did not result in significant HRP labeling compared with control (data

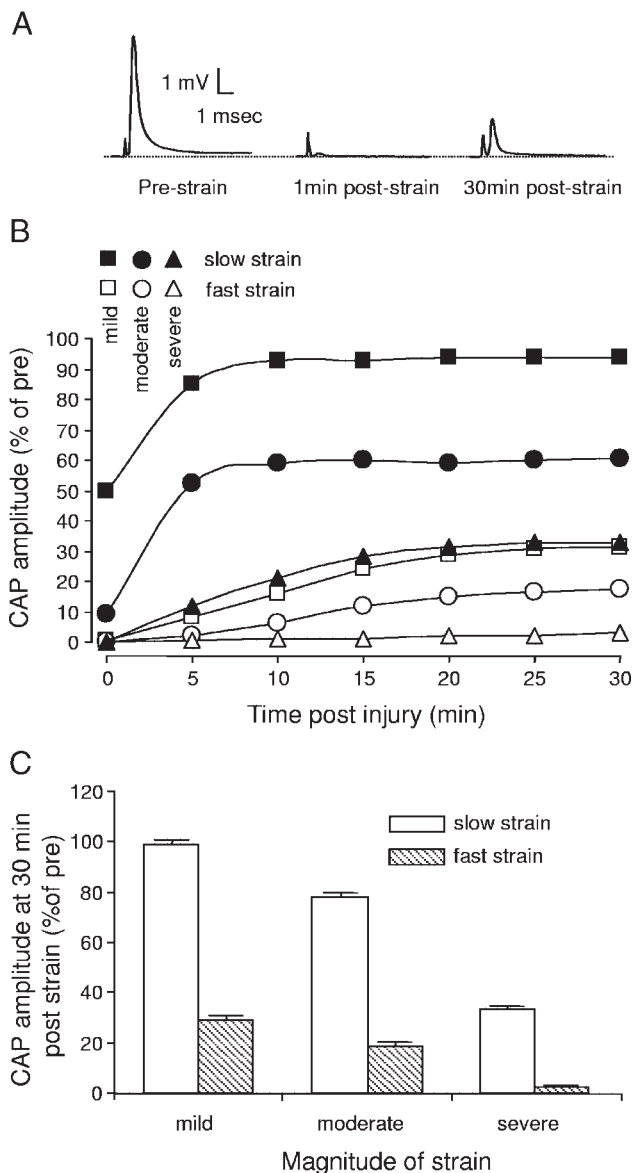


FIG. 2. Graph showing the change in compound action potential (CAP) amplitude after strain. *A*: samples of loss and partial recovery of CAP in response to strain (fast-mild strain). *B*: 6 cases indicating varying degrees of conduction loss after strain. Filled symbols represent preparations subjected to slow strain (strain rate:  $0.006\text{--}0.008\text{ s}^{-1}$ ). Open symbols represent fast strain (strain rate:  $355\text{--}519\text{ s}^{-1}$ ). Square symbols signify preparations suffering mild strain (25%), circles denote moderate strain (50%), and triangles stand for severe strain (100%). *C*: average percentage of CAP amplitude lost after strain at various injury levels. In each case, slow or fast strain, higher magnitudes of strain significantly reduced CAP amplitude compared with lower magnitudes ( $P < 0.05$ ). Similarly, in each magnitude, fast strain consistently inflicted more functional injury compared with slow strain ( $P < 0.01$ ).

not shown). The quantification of HRP labeling in the fast-severe strain group was not performed because of the poor quality of the tissue sample. No significant HRP labeling were found in slow-mild strain group.

#### Nonselectivity of small and large diameter axons to strain injury

The differential susceptibility of large and small axons to strain was studied both physiologically and anatomically. As

shown in Fig. 4, an electrophysiological measurement, a current-voltage test, was performed before and 30 min after injury in fast-mild strain (Fig. 4). A comparison of the response amplitude, before and 30 min after strain, to a set of stimulus voltages (1.85–6.5 V) showed no significant difference in the relative decrease of amplitude at different stimulus intensities over a wide range. Figure 4 shows data from six different cord specimens that were stimulated at similar intensities before and 30 min after strain and compared in absolute terms (as a percentage of the maximal amplitude). The near unity slope of the relation indicates there was no consistent selectivity in the loss of conductivity in fibers with low or high thresholds in response to strain. Similar tests were conducted in fast-moderate, slow-moderate, and slow-severe groups and no preferential vulnerability of axonal damage based on caliber was found (data not shown).

We further studied the issue of differential vulnerability of axons to strain as a function of caliber by using an HRP exclusion test. Figure 5 shows the HRP labeling in percentage (percent of overall axonal population) of both background (immediate posttransection) and at 30 min after strain (fast-moderate). There is no significant difference between these two groups in all five axon caliber groups ( $P > 0.05$ ). This indicates that axon populations of different calibers respond proportionally to strain or the diameter of axons did not influence their susceptibility to strain when membrane permeability is used as an indicator of axonal damage. Similar results were also obtained in fast-mild, slow-moderate, and slow-severe groups. This is consistent with the electrophysiological data suggesting that there is no differential vulnerability of axons with different diameters to strain injury.

## DISCUSSION

### *Ex vivo strain model*

The current *ex vivo* strain model is unique compared with other cell culture nerve strain models (Ellis et al. 1995; Geddes et al. 2003; Smith et al. 1999). This type of preparation preserves the local environment that likely affects the behavior of each single axon under strain. These factors will certainly influence the biomechanics of axons when the cord is deformed from an external load. We believe the information derived from this model is likely to be a valuable supplement to the existing *in vitro* models (Ellis et al. 1995; Geddes et al. 2003; Smith et al. 1999).

Unlike *in vivo* models, this *ex vivo* model is also capable of separating ischemic injury from mechanical insult (Peasley and Shi 2002; Shi and Pryor 2002). It is also possible to perform strain injury of various magnitudes and strain rates. To our knowledge, this is the first time that an *ex vivo* preparation of spinal cord segments was subjected to controlled strain with different magnitudes and strain rates. We believe that this method could also serve as a valuable supplement to existing *in vivo* models of strain injury (Jafari et al. 1997, 1998).

Despite the advantages of this model, it is unclear the correlation, if any, of our experimental findings to precise clinical situations. Rather, the results must be interpreted as a study of the basic biomechanical response of spinal cord tissue over an extreme range of strains and strain rates. It is our expectation that such knowledge may contribute to the im-

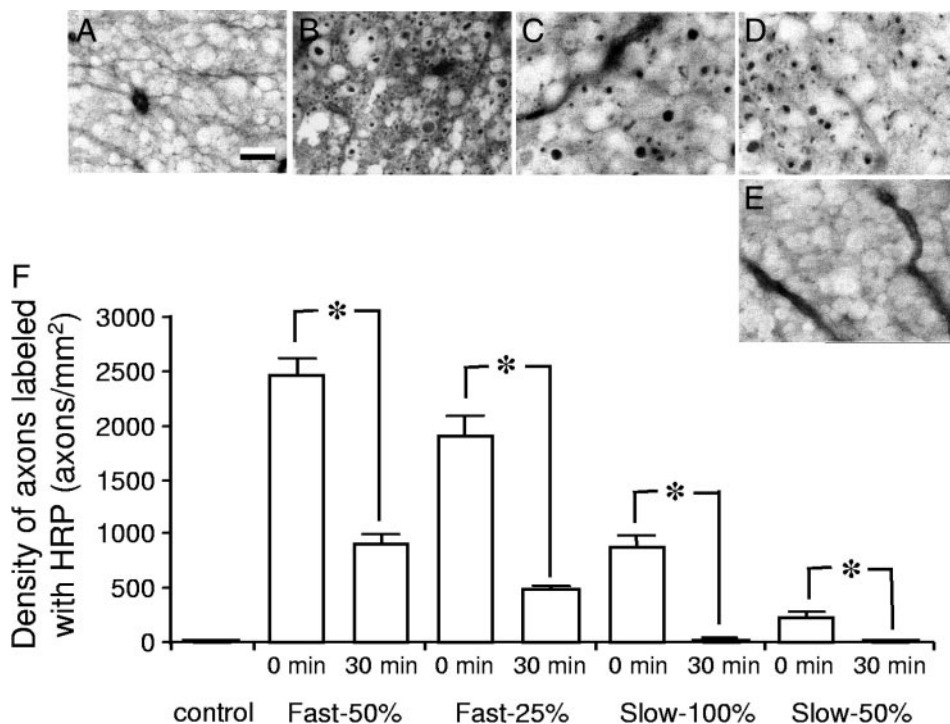


FIG. 3. Photographs of vibatome sections showing horseradish peroxidase (HRP) labeling and quantification under different conditions. Micrographs from 5 groups represent control (uninjured) (A), fast-mild strain at 0 min (B), fast-mild strain at 30 min (C), slow-severe strain at 0 min (D), and slow-severe strain at 30 min (E). F: quantification of HRP-labeled guinea pig spinal cord axons under different conditions. Note that increased magnitude of strain or the speed of the strain (strain rate) consistently increases membrane damage. Note also that significant spontaneous recovery is evident in all conditions within 30 min after strain ( $*P < 0.01$ ). Scale bar = 10  $\mu\text{m}$  (applies to A–E).

proved understanding of white matter tissue in response to mechanical deformation.

#### Axonal damage is sensitive to both magnitude and the rate of strain

Using this *ex vivo* spinal cord injury model, we have found that axonal damage is proportional to the magnitude of strain. In addition, it is also clear that axons are sensitive to strain rate, a phenomenon previously shown in tissue culture (Galbraith et al. 1993; Geddes et al. 2003). In this study, at a strain magnitude of 25%, slow strain caused little axonal membrane damage, if any, while fast strain compromised membrane integrity in almost 70% of the axons. Similarly, slow-mild (25%) strain caused no irreversible CAP amplitude loss, whereas fast strain resulted in about 70% of CAP amplitude loss when monitored

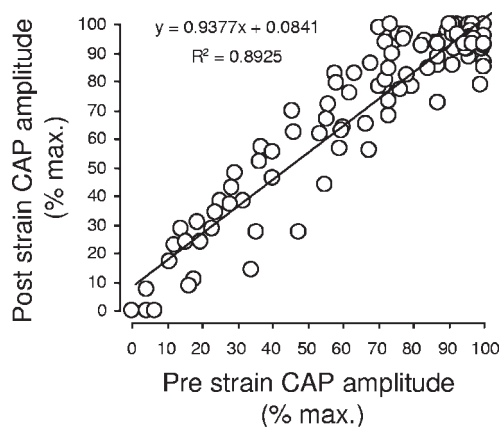


FIG. 4. Normalized CAP amplitude before strain (fast 25%), which is plotted against the CAP amplitude 30 min after strain at the same stimulus intensities for 6 cord strips. Stimulus intensity ranged from 1.85 to 6.5 V. Overall trend reveals a linear relationship suggesting there is little difference in susceptibility of axons with different activation thresholds to strain injury.

at 30 min after injury. One interesting comparison that further highlights the importance of strain rate is that a mild fast strain (25%) inflicted more axonal damage, both structurally and functionally, than a severe (100%) but slow strain.

There is one point worth mentioning that is related to the variability of strain rate within the fast group. Because the strain rate increases considerably with strain magnitude (e.g., from  $355 \text{ s}^{-1}$  at 25% to  $519 \text{ s}^{-1}$  at 100%), it is likely that the increase in injury is not solely caused by increase in strain, but strain rate may also play a role. The other interesting point is that at a strain rate of around  $0.008 \text{ s}^{-1}$  (slow strain), a 100%

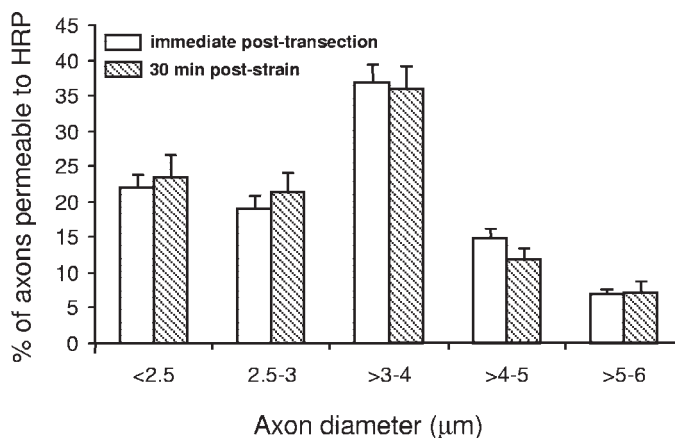


FIG. 5. Comparison of the percentage of population of each axon caliber group in 2 conditions (immediate posttransection and 30 min after strain). Each group is expressed as a percentage of the total labeled axons evaluated. Note that if axons of the different caliber groups were equally susceptible to strain, there would not be any statistical difference between the percent of axons in background (immediate posttransection) and those damaged because of strain (30 min after strain). Bar graphs show no statistical differences between the percent of axons in transection and strained group in any of the caliber groups ( $P > 0.05$ ). This indicates that the strain injury does not favor 1 range of axon diameters over another.

strain could still leave 30% of the CAP amplitude (compared with preinjury) remaining and result in almost no axons permeable to HRP when examined 30 min after injury. This indicates that cord tissue can tolerate a relatively severe strain if the speed of loading is slow. This finding may be informative in both diagnosis as well as treatment of spinal cord injury.

#### *Significance of HRP labeling*

The molecular weight of HRP, a compound used in this study to denote the integrity of the axonal membrane, is 44 kDa. The size of membrane holes that allow the passage of HRP is estimated to be ~5 nm (Oliver et al. 1992; Shimizu and Kawazoe 1996). Therefore it is important to bear in mind that a disruption smaller than the size of HRP will go undetected by HRP. Therefore the assessment of membrane disruption based on HRP labeling could be, to a certain degree, an underestimation compared with evaluations using smaller molecules. A more complete estimation may require a combination of several compounds with various diameters (Luo et al. 2002). Nevertheless, considering a reasonably good correlation of HRP labeling with the functional measurements of axonal membrane (Shi and Pryor 2000), the HRP exclusion test still offers a fairly effective picture of membrane integrity.

#### *Spontaneous recovery of action potential and membrane integrity*

Our findings indicate that axons subjected to strain have spontaneous recovery both anatomically and functionally. Interestingly, such spontaneous membrane repair in fast strain is incomplete when examined at 30 min after injury. For example, there are still significant amounts of HRP labeling 30 min after fast strain at both mild and moderate injuries. Longer periods of observations show that there is no further significant recovery between 30 min and up to 2 h after injury (data not shown). These data indicate that the speed of resealing after strain is slower than that of transected cord, which sealed most of its axons at 30 min after injury (Shi et al. 2000). The reason for this discrepancy is not fully established. One likely explanation is simply the length of the axons affected by transection or strain. While transection is seemingly a more dramatic injury, it only affects one plane of the axons. On the other hand, although the cord is not completely severed, strain may affect a longer segment of the axons (~5 mm in this study). Therefore the injury site may be more diffuse in strain and involve multiple membrane disruptions. In turn, this could prolong the resealing times. This argument is speculative as the detailed biomechanics of how the plasma membrane of an axon breaks down under an external load is not established. Extrapolating this knowledge requires an understanding of cellular and molecular biomechanics of axons and how the external force is transferred onto the axonal lipid bilayer. It is likely that establishment of this mechanism will greatly advance our knowledge of axonal membrane damage. Nonetheless, it is well known that the sooner the disrupted axonal membrane is sealed, the better the probability of cell survival and proper function. Therefore the slower resealing time suggests strained axons may have decreased survival rates than transected axons.

#### *Heterogeneity of axonal injury: the factor of location and size*

Because the response of axons to strain is heterogeneous in terms of membrane leakage, it would be interesting to know what key factor(s) influence axonal membrane damage. One possible contributor is the location of the axons. Because of the characteristic shape of the cord strips, roughly a cylinder, it has been shown that the axons within the cord strips would experience the load (strain) differently based on their location (Shi and Pryor 2002). Previous studies suggest that axons in the middle of the nerve bundle may be strained less while the axons in the outer realm of the nerve suffer more during a longitudinal strain (Shi and Pryor 2002). Indeed, preliminary studies have confirmed this speculation that axons in the outer realm are likely to experience more elongation in strain injury (Shi and Pryor 2002).

In contrast to axonal location, we have found that the size of axon plays no significant role in the susceptibility of axons to strain. Based on both electrophysiological analysis and anatomical evaluations, we conclude that acute strain inflicts damage that did not correlate with axonal caliber in guinea pig spinal cord. This is also consistent with the observation in acute compression injury using this *ex vivo* model (Shi and Blight 1996; Shi and Borgens 1999). Taken together, it may be a general rule that the size may not affect the susceptibility of axons to pure mechanical trauma. It is interesting to note that the large axons are more vulnerable to oxygen and energy deprivation using the same preparation (Peasley and Shi 2002). Therefore a selective vulnerability of axons to mechanical insults based on their caliber seen *in vivo* (Blight 1991; Blight and DeCrescito 1986; Jafari et al. 1997, 1998) may result from true secondary pathological mechanisms and perhaps a selective metabolic susceptibility of certain axons or axons in certain environment.

#### ACKNOWLEDGMENTS

We thank M. A. Logan and P. Zickmund for invaluable assistance during the course of this project and J. Li, J. McBride, and P. Zickmund for critical reading of the manuscript.

#### GRANTS

This study was supported by funding from the National Institutes of Health and the State of Indiana. J. Whitebone was supported by a Research Fellowship from Merck Pharmaceutical.

#### REFERENCES

- Anderson DK and Hall ED. Pathophysiology of spinal cord trauma. *Ann Emerg Med* 22: 987–992, 1993.
- BeMent SL and Ranck JB Jr. A quantitative study of electrical stimulation of central myelinated fibers. *Exp Neurol* 24: 147–170, 1969.
- Blight AR. Mechanical factors in experimental spinal cord injury. *J Am Paraplegia Soc* 11: 26–34, 1988.
- Blight AR. Morphometric analysis of a model of spinal cord injury in guinea pigs, with behavioral evidences of delayed secondary injury. *J Neurol Sci* 103: 156–171, 1991.
- Blight AR and DeCrescito V. Morphometric analysis of experimental spinal cord injury in the cat: the relation of injury intensity to survival of myelinated axons. *Neuroscience* 19: 321–341, 1986.
- Ellis EF, McKinney JS, Willoughby KA, Liang S, and Povlishock JT. A new model for rapid stretch-induced injury of cells in culture: characterization of the model using astrocytes. *J Neurotrauma* 12: 325–339, 1995.
- Fiford RJ, Bilston LE, Waite P, and Lu J. A vertebral dislocation model of spinal cord injury in rats. *J Neurotrauma* 21: 451–458, 2004.

- Galbraith JA, Thibault LE, and Matteson R.** Mechanical and electrical responses of the squid giant axon to simple elongation. *J Biomech Eng* 115: 13–22, 1993.
- Geddes DM, Cargill RS II, and LaPlaca MC.** Mechanical stretch to neurons results in a strain rate and magnitude-dependent increase in plasma membrane permeability. *J Neurotrauma* 20: 1039–1049, 2003.
- Honmou O and Young W.** Traumatic injury of spinal axons. In: *The Axon*, edited by Waxman SG, Kocsis JD, and Stys PK. New York: Oxford, 1995, p. 480–529.
- Jafari SS, Maxwell WL, Nielson M, and Graham DI.** Axonal cytoskeletal changes after non-disruptive axonal injury. *J Neurocytol* 26: 207–221, 1997.
- Jafari SS, Nielson M, Graham DI, and Maxwell WL.** Axonal cytoskeletal changes after nondisruptive axonal injury. II. Intermediate sized axons. *J Neurotrauma* 15: 955–966, 1998.
- Jensen JM and Shi R.** Effects of 4-aminopyridine on stretched mammalian spinal cord: the role of potassium channels in axonal conduction. *J Neurophysiol* 90: 2334–2340, 2003.
- Kandel ER, Schwartz JH, and Jessell TM.** *Principles of Neural Science*. New York: McGraw-Hill, 2000.
- Luo J, Borgens RB, and Shi R.** Polyethylene glycol immediately repairs neuronal membranes and inhibits free radical production after acute spinal cord injury. *J Neurochem* 83: 471–480, 2002.
- Oliver JD III, Anderson S, Troy JL, Brenner BM, and Deen WH.** Determination of glomerular size-selectivity in the normal rat with Ficoll. *J Am Soc Nephrol* 3: 214–228, 1992.
- Peasley MA and Shi R.** Resistance of isolated mammalian spinal cord white matter to oxygen-glucose deprivation. *Am J Physiol Cell Physiol* 283: C980–C989, 2002.
- Shi R.** The dynamics of axolemmal disruption in guinea pig spinal cord following compression. *J Neurocytol* 33: 203–211, 2004.
- Shi R, Asano T, Vining NC, and Blight AR.** Controls of membrane sealing in injured mammalian spinal cord axons. *J Neurophysiol* 84: 1763–1769, 2000.
- Shi R and Blight AR.** Compression injury of mammalian spinal cord in vitro and the dynamics of action potential conduction failure. *J Neurophysiol* 76: 1572–1580, 1996.
- Shi R and Borgens RB.** Acute repair of crushed guinea pig spinal cord by polyethylene glycol. *J Neurophysiol* 81: 2406–2414, 1999.
- Shi R and Pryor JD.** Temperature dependence of membrane sealing following transection in mammalian spinal cord axons. *Neuroscience* 98: 157–166, 2000.
- Shi R and Pryor JD.** Pathological changes of isolated spinal cord axons in response to mechanical stretch. *Neuroscience* 110: 765–777, 2002.
- Shimizu N and Kawazoe Y.** A new method for permeabilization of the plasma membrane of cultured mammalian cells. III. Internalization of fluorescent dextrans into cultured mammalian cells by vortex-stirring in the presence of high molecular weight polyacrylic acid. *Biol Pharm Bull* 19: 1023–1025, 1996.
- Smith DH, Wolf JA, Lusardi TA, Lee VM, and Meaney DF.** High tolerance and delayed elastic response of cultured axons to dynamic stretch injury. *J Neurosci* 19: 4263–4269, 1999.
- West DC and Wolstencroft JH.** Strength-duration characteristics of myelinated and non-myelinated bulbospinal axons in the cat spinal cord. *J Physiol* 337: 37–50, 1983.